

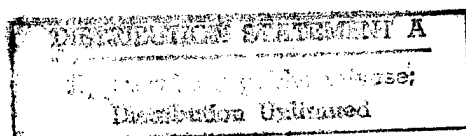
2 SEP 1998

**AASERT Annual Report****Fuel/Air Mixing and Flame Structure Measurements for  
Advance Low Emission Gas Turbine Combustors****Timothy R. Frazier, Robert E. Foglesong, Robert E. Coverdill,  
James E. Peters, and Robert P. Lucht**

Department of Mechanical and Industrial Engineering  
University of Illinois at Urbana-Champaign  
1206 W. Green St.  
Urbana, IL 61801

Grant No. F49260-97-1-0456

September 1, 1998



19980918 011

DTIC QUALITY INSPECTED 1

## REPORT DOCUMENTATION PAGE

Form Approved  
OMB No. 0704-0188

Public reporting burden for this collection of information is estimated to average 1 hour per response, including the time for reviewing instructions, searching existing data sources, gathering and maintaining the data needed, and completing and reviewing the collection of information. Send comments regarding this burden estimate or any other aspect of this collection of information, including suggestions for reducing this burden, to Washington Headquarters Services, Directorate for Information Operations and Reports, 1215 Jefferson Davis Highway, Suite 1204, Arlington, VA 22202-4302, and to the Office of Management and Budget, Paperwork Reduction Project (0704-0188), Washington, DC 20503.

1. AGENCY USE ONLY (Leave blank)		2. REPORT DATE September 1, 1998	3. REPORT TYPE AND DATES COVERED Annual Technical Report August 1, 97 July 31, 98	
4. TITLE AND SUBTITLE (U) Fuel/Air Mixing and Flame Structure Measurements for Advanced Low Emission Gas Turbine Combustors			5. FUNDING NUMBERS PE - 61103D PR - 3484 SA - WS G - F49620-97-1-0456	
6. AUTHOR(S) Timothy R. Frazier, Robert E. Foglesong, Robert E. Coverdill, James E. Peters, and Robert P. Lucht				
7. PERFORMING ORGANIZATION NAME(S) AND ADDRESS(ES) University of Illinois Department of Mechanical and Industrial Engineering 1206 W. Green St. Urbana, IL 61801			8. PERFORMING ORGANIZATION REPORT NUMBER	
9. SPONSORING/MONITORING AGENCY NAME(S) AND ADDRESS(ES) AFOSR/NA 110 Duncan Avenue, Suite B115 Bolling AFB DC 20332-0001			10. SPONSORING/MONITORING AGENCY REPORT NUMBER	
11. SUPPLEMENTARY NOTES				
12a. DISTRIBUTION/AVAILABILITY STATEMENT Approved for public release; distribution is unlimited			12b. DISTRIBUTION CODE	
13. ABSTRACT (Maximum 200 words)  A gas turbine combustion facility with optical access was developed which allows the use of laser diagnostic techniques to measure temperature and species concentrations within the combustion zone. The mixing effectiveness of a dual annular counter-rotating swirler premixer was examined using planar laser-induced fluorescence (PLIF) of acetone-seeded gaseous fuel to provide quantitative maps of the spatial and temporal fuel/air distributions emanating from the premixer. Time-averaged results showed maximum spatial variations on the order of 50% of the known overall equivalence ratio. Temporal unmixedness resulted in peak equivalence ratios 2.4 times greater than the overall stoichiometry.				
14. SUBJECT TERMS Gas Turbine Combustion, Fuel/Air Mixing, Emissions			15. NUMBER OF PAGES	
			16. PRICE CODE	
17. SECURITY CLASSIFICATION OF REPORT Unclassified	18. SECURITY CLASSIFICATION OF THIS PAGE Unclassified	19. SECURITY CLASSIFICATION OF ABSTRACT Unclassified	20. LIMITATION OF ABSTRACT UL	

# TABLE OF CONTENTS

	Page
1.0 Status of Effort .....	1
2.0 Accomplishments.....	1
2.1 Combustion Tunnel Design and Operation.....	1
2.2 Laser Diagnostics.....	4
2.3 Cold Flow Mixing Studies .....	5
2.3.1 Cold Flow Mixing Studies: 100 kPa.....	5
2.3.1.1 Time-Averaged PLIF Results.....	8
2.3.1.2 Single-Shot PLIF Results.....	12
2.3.2 Cold Flow Mixing Studies: 500 kPa.....	18
2.4 Conclusions and Future Efforts.....	22
2.4.1 Conclusions.....	22
2.4.2 Future Efforts .....	22
2.5 References .....	23
3.0 Personnel.....	23
4.0 Publications .....	23
5.0 Interactions/Transitions.....	23
6.0 Discoveries, Inventions and/or Disclosures .....	24
7.0 Honors/Awards .....	24

## **1.0 Status of Effort**

During the past year, a study of the fuel/air mixing process downstream of a dual-annular counter-rotating swirler premixer was initiated. Atmospheric-pressure fuel/air mixing studies were completed. High-pressure mixing studies are underway. A complete description of the facility and the results of a comprehensive set of acetone planar laser-induced fluorescence (PLIF) fuel/air mixing images are included in this report. Studies of the premixer performance near atmospheric pressure show significant spatial and temporal fluctuations in fuel concentration as the flow leaves the premixer. Shakedown combustion tests have also been completed and planar OH laser diagnostic images of the reacting flow will begin in the near future.

## **2.0 Accomplishments**

A gas turbine combustion facility with optical access was developed which allows the use of laser diagnostic techniques to measure temperature and species concentrations within the combustion zone. Details of the combustion tunnel and diagnostic tools relevant to PLIF and the results of a series of cold flow mixing studies are provided below.

### **2.1 Combustion Tunnel Design and Operation**

A schematic of the facility is shown in Fig. 1. Compressed, dry air is supplied from a tank farm and preheated by a non-vitiated natural gas burner. An upstream control valve regulates the inlet pressure supplied to the premixer. Air mass flowrate is measured by an orifice plate. Before entering the premixer, the flow passes through a flow conditioning section consisting of a series of screens and honeycomb. Hot wire measurements of the inlet flow to the premixer were performed to ensure uniformity, showing a variation in velocity of only 0.25% across the diameter of the premixer inlet at atmospheric flow conditions.

A schematic of the dual-annular counter-rotating swirler assembly as viewed from downstream is shown in Fig. 2. Gaseous fuel is injected axially from three holes located on the trailing edge of each outer swirling vane. Additionally, fuel is injected radially inward from a single port centered between each vane on the outer wall of the premixer manifold. The vane combination for these experiments is comprised of ten clockwise rotating (as viewed from downstream) outer swirlers with a vane angle of 45 degrees and five counter-clockwise inner swirlers with a vane angle of 55 degrees. Mixing of the fuel and combustion air occurs within the conical section of the axial premixer (see Fig. 3, a cutaway of the combustion section). The reduction in cross sectional area across the mixing duct is approximately 2:1 with the premixer exit diameter measuring 48 mm.

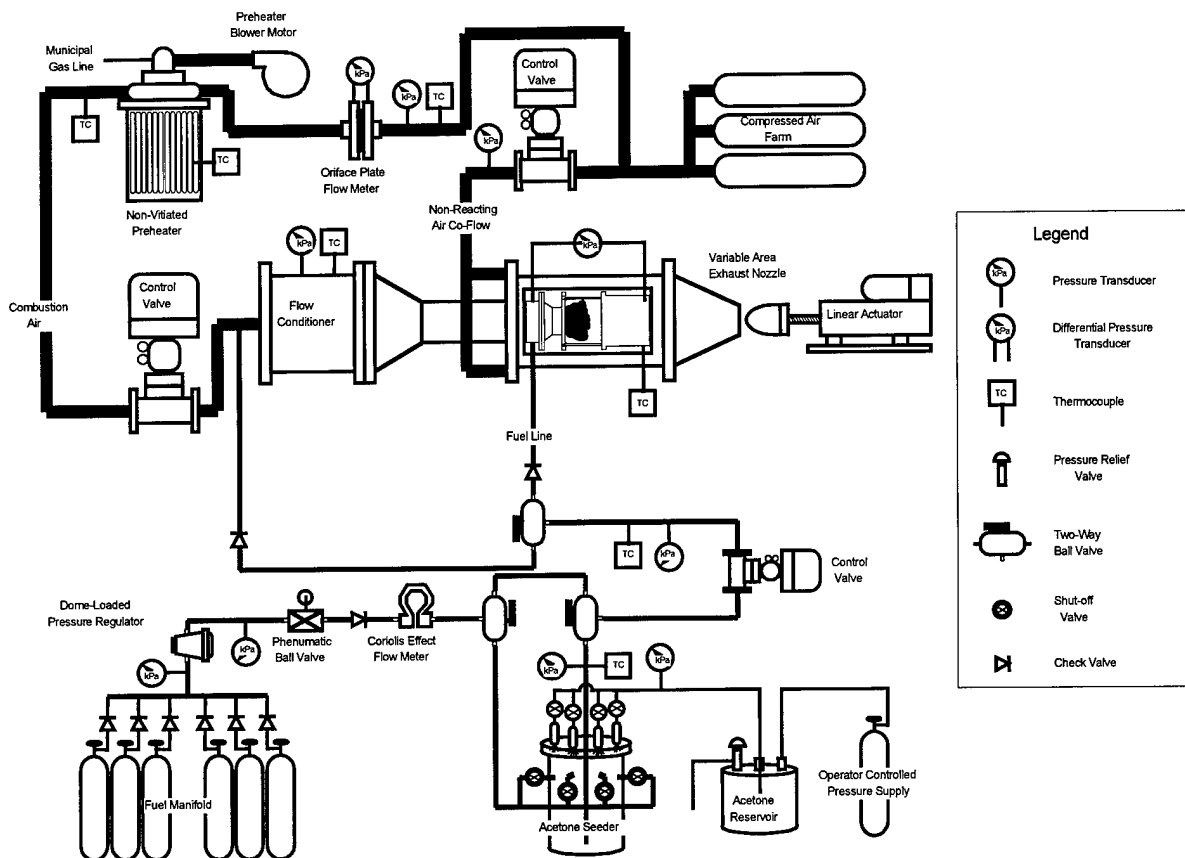


Figure 1. Experimental combustion facility for high-pressure and temperature flowfields.

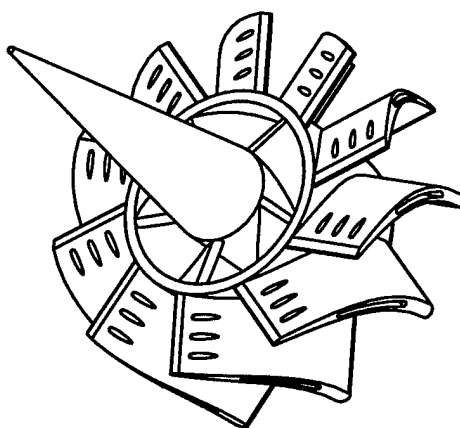


Figure 2. Dual-annular counter-rotating swirler assembly as viewed from downstream.

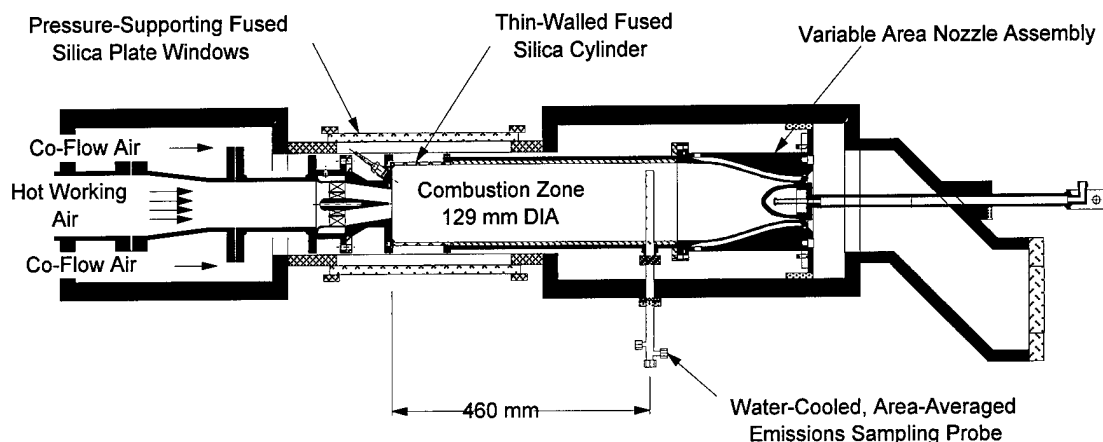


Figure 3. Sectional view of experimental combustor.

The increase in cross-sectional area from the premixer to the combustion zone is 7.2:1. Axial flow of the combustion gases remains unobstructed downstream of the premixer for approximately 3.5 diameters (0.5 m) of the circular combustion zone. At this location, the mixture of gases is exhausted through an axisymmetric cone and nozzle assembly, which at high operating pressures chokes the flow and, therefore, minimizes flow disturbances. This choking assembly, which is driven by a stepper motor linear actuator system, also provides control for the pressure drop across the combustor.

To prevent damage to the stainless steel components of the combustion chamber from the heat generated during combustion, water cooling channels have been added to the back face of the premixer, the combustion chamber, and the choking cone and nozzle. All of these cooling systems are fully enclosed to prevent disturbance of the combustion gases. Downstream of the choking assembly, water is injected to cool the exhaust gases.

As shown in Fig. 1 methane fuel is supplied from a six-cylinder manifold. The flowrate is measured by a Coriolis effect flowmeter and regulated by a pneumatic control valve. Combustion is initiated using a spark igniter located on the back face of the premixer exit. To prevent combustion downstream of the test section during the light-off process, which is performed at atmospheric pressure, dilution air is injected into the exhaust system to ensure that the equivalence ratio of the mixture in the exhaust section is below the lean flammability limit. As an additional safety precaution, water sprays are injected throughout the exhaust section. An ultraviolet flame detector monitors presence of the flame through the fused silica cylinder, approximately 4 cm downstream of the premixer exit.

Optical access to the combustion region is provided through a 129-mm-diameter by 101-mm-length thin-wall fused silica cylinder downstream of the premixer exit. A co-flow of cold

(298 K), non-reacting gas flows across the outside of the combustion chamber to provide the proper backside cooling. The pressure of the co-flow, which is continuously monitored and adjusted to match the pressure within the combustion zone, is contained by three one-inch-thick fused silica windows, providing complete optical access to the combustion region.

Upon completion of the gas turbine facility, comprehensive benchmarking was performed to determine the operational limitations of the facility. Due to pressure losses in the working air preheating system, the maximum operating pressure has been found to be approximately 6 atm. For near atmospheric supply temperatures, mass flow supply limitations of the air compressors reduce the sustainable air supply pressure to approximately 5 atm. Air temperature, air pressure, percent pressure drop across the combustor, and equivalence ratio are controlled automatically by a LabVIEW based data acquisition system and can be maintained to within  $\pm 20$  K,  $\pm 2.5\%$ ,  $\pm 6\%$  (relative), and  $\pm 0.03$  of their respective setpoints.

High speed (10 kHz) pressure transducer measurements were used to measure pressure fluctuations that occur during the combustion process. The maximum pressure fluctuations recorded were approximately 14 kPa, an order of magnitude lower than the burst pressure of the thin-wall fused silica cylinder. During combustion tests of up to 400 kPa, the water cooling systems proved capable of preventing any noticeable damage to the various components of the test section from the combustion generated heat flux.

Exhaust gas sampling can be accomplished with a water-cooled stainless steel sampling probe located approximately three combustor diameters downstream of the premixer. The continuous flow gas analysis equipment includes an NO/NO<sub>x</sub> chemiluminescent analyzer, CO and CO<sub>2</sub> non-dispersive infrared analyzers, a flame ionization detector HC analyzer, and a paramagnetic O<sub>2</sub> analyzer.

## 2.2 Laser Diagnostics

The gas turbine facility has been designed for detailed laser diagnostic investigations within the reaction zone of the combustor. Among the diagnostic techniques to be implemented are acetone and OH PLIF which will be used to quantitatively describe the fuel/air mixing process and qualitatively map the flame structure, respectively. The equipment that is available for these laser diagnostic techniques include two Nd:YAG lasers, two tunable narrowband dye lasers, and a broadband dye laser. Frequency-doubling crystals are used for doubling the visible frequencies of the narrowband dye lasers into the ultraviolet (UV) range for fluorescence measurements. All optical access ports are UV grade fused silica.

For these laser diagnostic measurements, automation of the data acquisition process for the laser diagnostic systems is critical due to the expense of running the combustion facility at high pressure for long periods of time. Consequently, all optical component translation systems are

fully automated through the LabVIEW system. The stepper-motor-driven stages provide automated vertical and axial translation allowing complete mapping, with point laser diagnostic measurements, of a vertical plane parallel to the centerline of the combustor for an axial distance of 6 mm to a distance of 75 mm downstream of the exit face.

Further integration with the computer control systems has been achieved with the laser diagnostic acquisition systems. The CCD camera utilized for acquisition of PLIF images are remotely operated from the control room and fully automated to reduce acquisition time. With the high fuel demands of the 3x combustor, this automation is essential for obtaining statistically relevant time-resolved data.

For the non-reacting fuel/air mixing studies using acetone PLIF, methane fuel is replaced with diatomic nitrogen to minimize the chance of undesired combustion due to laser ignition. The nitrogen flowrate is set so that the mass flowrate of nitrogen matches the mass flowrate of methane for the specified methane equivalence ratio. A high capacity acetone seeding vessel is integrated into the fuel line to provide a tracer molecule for PLIF. The system utilizes six industrial spray atomizers to inject the acetone into transverse fuel jets. For atmospheric-pressure mixing studies, acetone seed rates are maintained at approximately 10% of the mass flow of  $N_2$ . The acetone mixing chamber offers a wide range of potential seeding levels, which can easily be adjusted by changing the acetone supply pressure or turning individual nozzles on or off. To promote vaporization of the acetone in the fuel line, the acetone and fuel are heated upstream of the seeding chamber. The heated fuel supply line has been extended ( $L/D \approx 1000$ ) between the seeding chamber and the test section to ensure thorough mixing of the acetone and the fuel. The air flow is also maintained at an elevated temperature during fuel/air mixing studies to prevent condensation of the acetone upon injection of the fuel/acetone mixture into the air flow.

## 2.3 Cold Flow Mixing Studies

### 2.3.1 Cold Flow Mixing Studies: 100 kPa

The primary objective of the cold flow mixing studies is to quantitatively map the mixture equivalence ratio downstream of the dual-annular counter-rotating swirler premixer using instantaneous two-dimensional acetone PLIF images. In accordance with the literature, temporal fluctuations are quantified using the unmixedness parameter,  $s$ ,<sup>1</sup>

$$s = \frac{\sigma_\phi}{\mu_\phi} \quad (1)$$



where  $\mu_\phi$  and  $\sigma_\phi$  are the time-averaged mean and standard deviation of the local equivalence ratio, respectively. Flow conditions for the mixing experiments reported here are shown in Table 1.

Test Case Number	$P_{\text{comb}}$ (kPa)	$\Delta P_{\text{comb}}$ (%)	$\Phi_{\text{overall}}$	$T_{\text{comb}}$ (K)	$T_{\text{fuel}}$ (K)
I	116.0 $\pm 0.4$	3.2 $\pm 0.1$	0.70 $\pm 0.015$	427 $\pm 10$	305 $\pm 10$
II	116.0 $\pm 0.4$	3.0 $\pm 0.1$	0.40 $\pm 0.010$	390 $\pm 10$	310 $\pm 10$
III	116.0 $\pm 0.4$	5.2 $\pm 0.2$	0.69 $\pm 0.015$	350 $\pm 10$	305 $\pm 10$

Table 1. Atmospheric pressure test conditions.

To obtain quantitative fuel/air mixing results, the PLIF signal is calibrated at each operating condition. This is accomplished by diverting the seeded fuel flow to a distribution manifold in the combustion air supply upstream of the flow conditioner (see Fig. 1). The subsequent flow through the premixer is found to be a homogeneous mixture of fuel, oxidizer and acetone. By acquiring PLIF images for this configuration, the signal intensity is determined for a known equivalence ratio at conditions nearly identical to those in the subsequent mixing studies.

The PLIF system is shown schematically in Fig. 4. Acetone absorption is obtained by pumping molecules from the ground singlet state,  $S_0$ , to the first excited singlet state,  $S_1$ . The absorption is broadband, extending from 225 to 320 nm, and demonstrates a smooth peak between 270 and 280 nm. In this work, the excitation source is the frequency-quadrupled output (266 nm) of a Nd:YAG laser. This laser operates at a frequency of 10 Hz and is tuned to provide a 6-8 ns pulse of approximately 90 mJ. The planar beam is 30 mm wide and approximately 1 mm thick as it traverses the imaging region.

The fluorescence of the first excited singlet is a visible broadband spectrum ranging from 350 to 650 nm, with peaks at 445 and 480 nm. Breuer and Lee<sup>2</sup> measured an acetone fluorescence lifetime of  $1.7 \pm 0.3$  ns with 280 nm excitation source. This short lifetime, coupled with the short pulse of the Nd:YAG laser, effectively provides an instantaneous image of the flowfield and allows resolution of both spatial variations and temporal unmixedness simultaneously.

At the flow conditions used in this experiment, the fluorescence quantum efficiency of the first excited singlet state of the acetone molecule is nearly independent of molecular collisions.

This is because intersystem crossing to the first excited triplet state ( $T_3$ ) is the dominant relaxation mechanism.<sup>3</sup> The LIF signal from the first excited singlet state is fairly insensitive to temperature, pressure and local mixture composition.<sup>4</sup> While pressure and mixture concentrations are the same for the mixing studies and the corresponding calibration images, the temperature difference between the fuel supply and combustion air could affect the ratio of fluorescence signal intensities between the mixing and calibration results. Thurber et al.<sup>5</sup> investigated the temperature dependence of acetone fluorescence signals excited by 266 nm wavelengths. Their work indicates that at the maximum temperature difference of 100 K, the calibration error is on the order of 25%. However, additional heating of the fuel undoubtedly occurs within the fuel manifold during the mixing studies. Therefore, this represents a conservative upper limit on the error for the equivalence ratio determined in our mixing studies.

The PLIF images are acquired using a 512x512-pixel-array, 14-bit digital CCD camera. A Nikkor 50 mm glass lens with an  $f\#$  of 1.2 is used in conjunction with a lens-mounted macro extension tube to improve the signal-to-noise ratio and increase the magnification. Shutter control of the camera is maintained by networking to a personal computer. Average background signals are subtracted from the acetone images to eliminate any repeatable beam scattering. Images are then corrected for beam attenuation and normalized by an average of the homogenous calibration images to account for laser sheet non-uniformity.

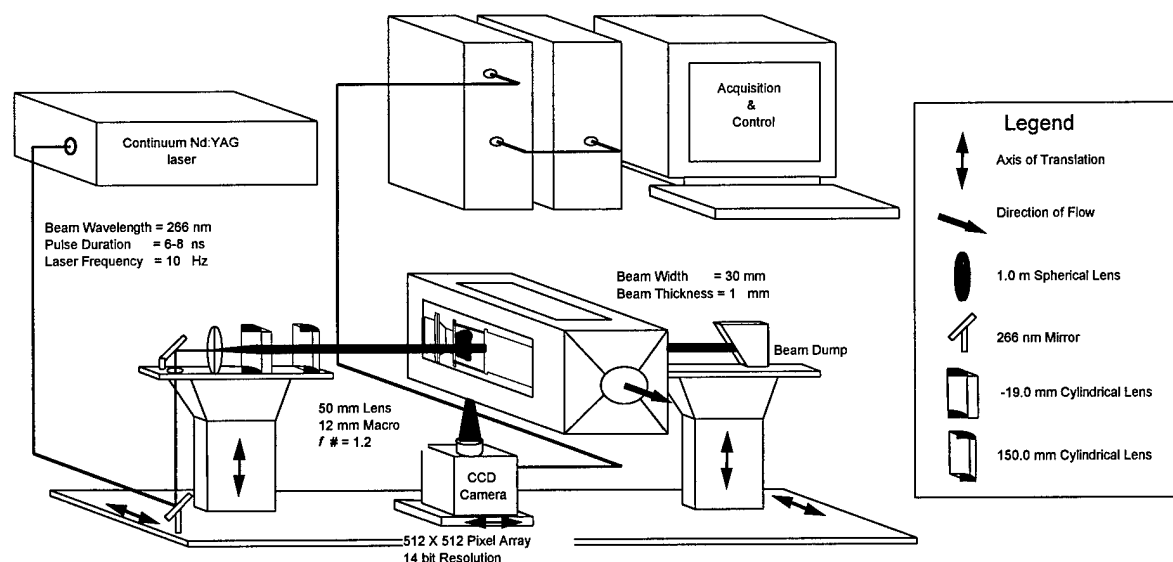


Figure 4. Layout of acetone PLIF optical setup and imaging equipment.

By translating the planar laser beam downstream of the premixer, two 30-mm portions of the flowfield can be probed. To improve spatial resolution, the camera is focused on one quarter of the desired mixing plane. The camera is then independently translated in the radial direction to collect two fluorescence images at each axial location. Figure 5 shows the assembly of the four image regions. Two images (regions 1 and 2) are centered about the axial centerline of the premixer and extend just beyond the edge of the premixer exit cone. Image regions 3 and 4 extend from the axial centerline radially to the outer edge of the combustor.

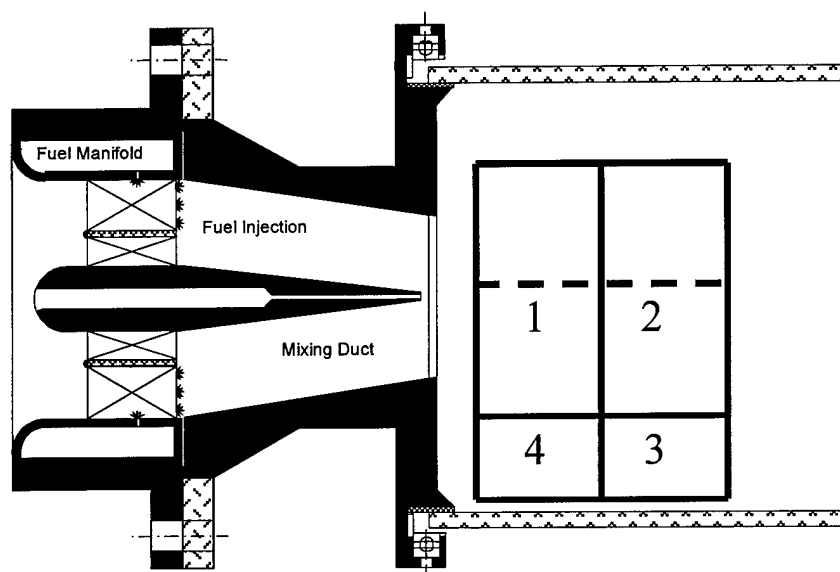


Figure 5. Image regions for acetone PLIF.

### 2.3.1.1 Time-Averaged PLIF Results

Figures 6, 7 and 8 show the time-averaged mixing results of acetone PLIF measurements at test conditions I, II and III, respectively. These 60-laser-shot averages were obtained by combining three sets of 20-shot exposures. The four regions of interest were then assembled to form Figs. 6a-8a. The line plots shown in Figs. 6b-8b were derived from the 60-shot averages. These graphs display the decay of spatial variations in the axial direction across the extent of the premixer exit cone. Statistical analysis performed on multiple 60-shot averages resulted in a pixel-to-pixel variation of only 5% of the local mean. This indicated that a 60-shot ensemble was sufficient to provide accurate time-averaged mixing results.

At each of the three test conditions, the time-averaged mixing results indicated that a fuel-rich annulus emanated from the premixer cone. The largest spatial variation in the fuel/air

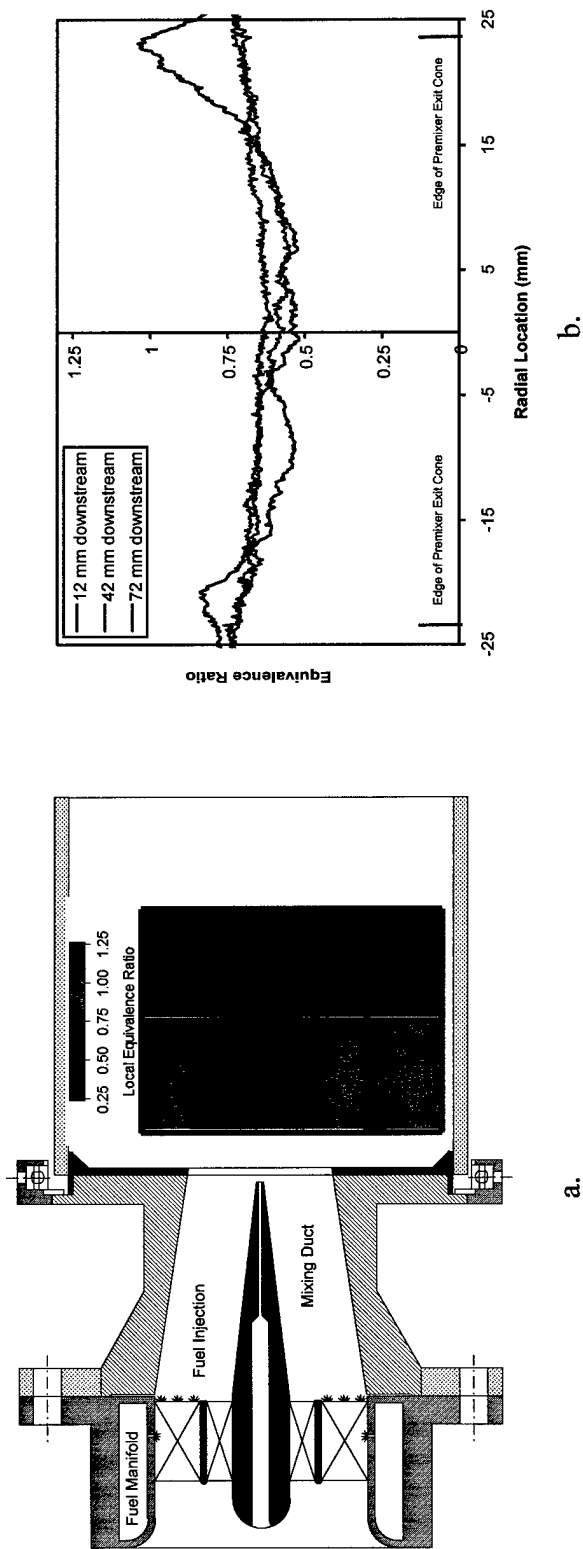


Figure 6. Acetone PLIF results for case I: a. Assembly of four 60-shot averages, b. Line profiles at three axial locations.

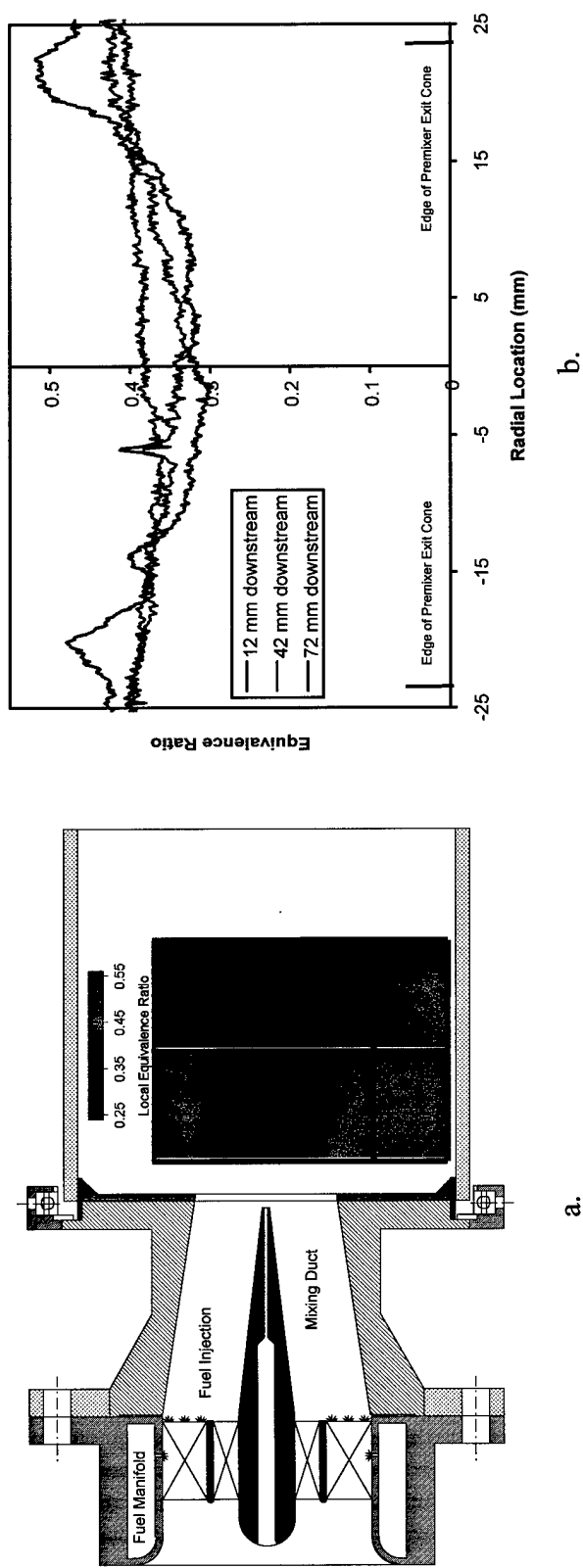


Figure 7. Acetone PLIF results for Case II: a. Assembly of four 60-shot averages, b. Line profiles at three axial locations.

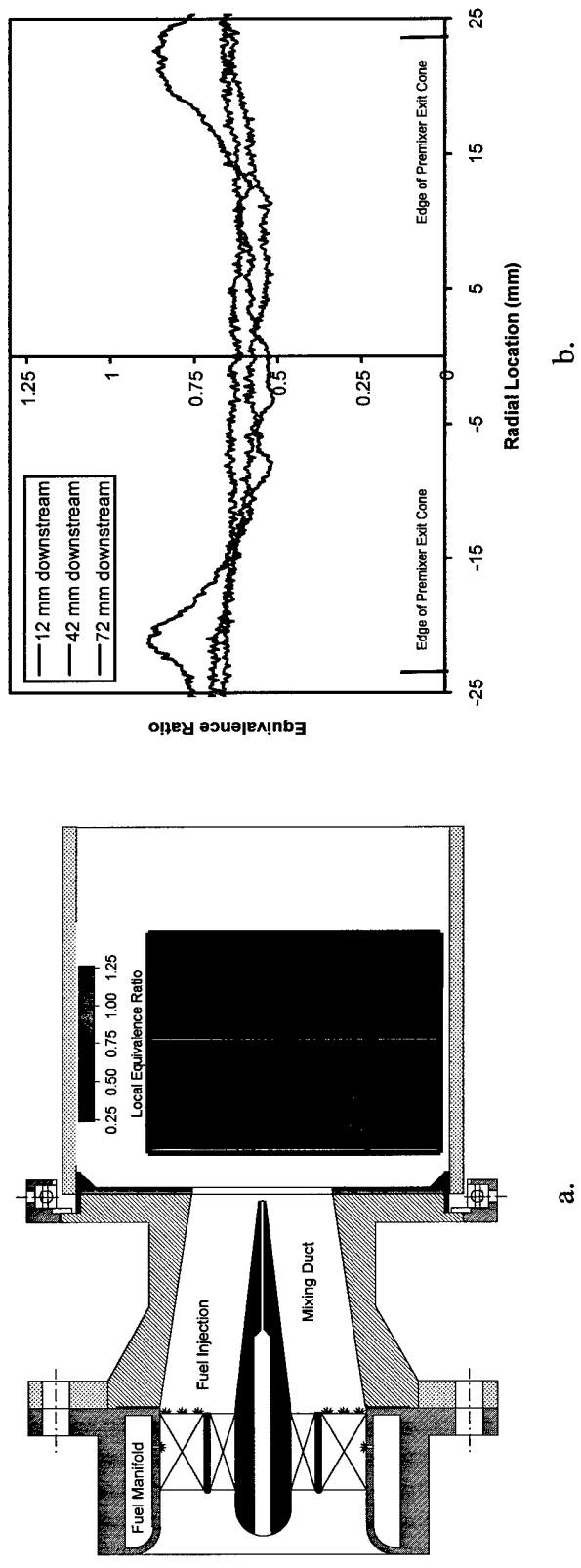


Figure 8. Acetone PLIF results for case III: a. Assembly of four 60-shot averages, b. Line profiles at three axial locations.

distribution resulted from test condition I where the combination of low air flowrate (3% pressure drop) and high equivalence ratio (0.7) produced a local maximum 51% greater than the overall equivalence ratio. This variation was greatly reduced at axial distances of 42 mm or greater from the premixer exit. However, a 0.1 variation in the local equivalence ratio across the radius of the premixer was still discernible 72 mm downstream of the premixer exit face.

Figure 7 shows that a reduction in the overall equivalence ratio to 0.4 improved the performance of the premixer. At this test condition, the local maximum was only 30% greater than the overall equivalence ratio. The line plot 72 mm downstream of the premixer reveals a nearly uniform mixture concentration.

Comparing the results shown in Fig. 8 with those displayed in Fig. 6 indicates that an increase in the air flowrate to produce a 5% pressure drop improved the mixing. In fact, the combination of high air flowrate and high equivalence ratio used in test case III resulted in the best mixing. At this condition the local maximum equivalence ratio was only 24% greater than the overall equivalence ratio. The mixture was nearly homogeneous at the 42 mm axial station.

Overall, the mixing results from the three test conditions show nearly an order of magnitude decrease in time-averaged spatial variations within an axial distance of 1.5 premixer exit diameters. The flowfield consistently showed good radial symmetry. Also, for each test condition, a mixture concentration uniform to within 8% of the overall equivalence ratio was observed in the recirculation zones in regions 3 and 4.

### 2.3.1.2 Single-Shot PLIF Results

While the time-averaged PLIF images provide a convenient mechanism for analyzing steady flow structures, phenomenological understanding of the effect of unmixedness on  $\text{NO}_x$  generation and flame stability requires resolution of both spatial and temporal fluctuations. Figures 9, 10 and 11 show instantaneous fuel/air distributions acquired from single-shot acetone PLIF images at test conditions I, II and III, respectively. The images are shown here as an assembly for the sole purpose of identifying their regional location. Each image in the assembly of four instantaneous snap-shots was acquired at the locations shown in Fig. 5. The images shown for locations 1-4 were not acquired simultaneously. Figures 12, 13 and 14 show the point histograms acquired from the single-shot acetone PLIF images at test conditions I, II and III, respectively. The results of a statistical analysis are shown on each histogram plot. The mean equivalence ratio is stated in terms of the 95% confidence interval. The center value of this interval and the local standard deviation were then used to calculate the temporal unmixedness parameter,  $s$ .

At each of the three test conditions, the single-shot PLIF results show a highly turbulent flowfield dominated by large-scale structures. Pockets containing fuel-rich mixtures emanate

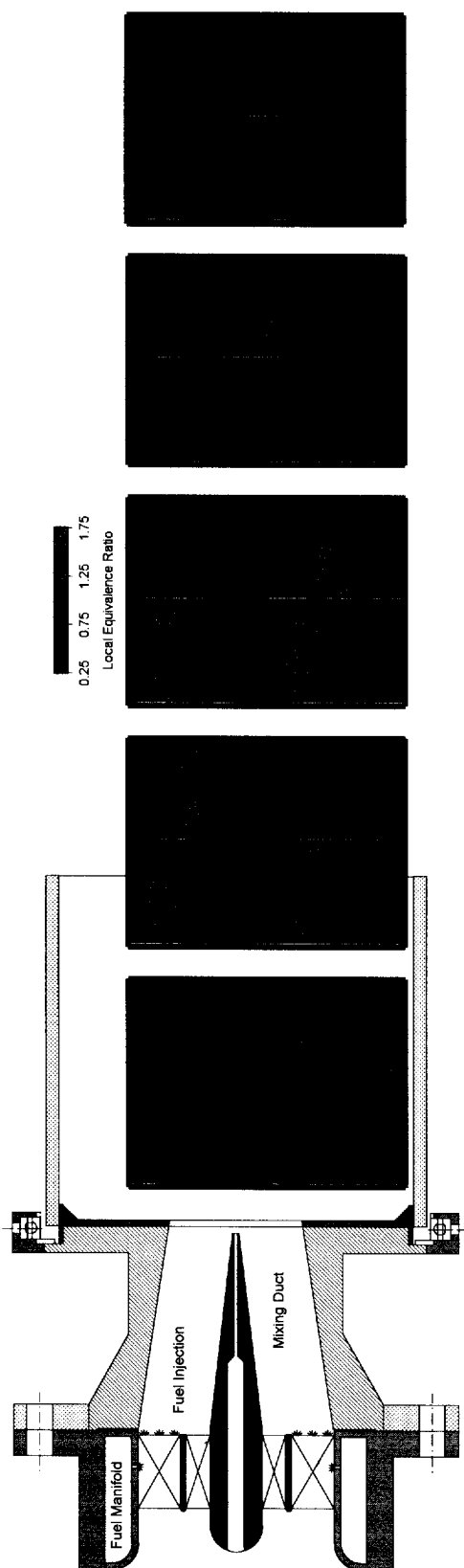


Figure 9. Assembly of four single-shot acetone PLIF results for case I.

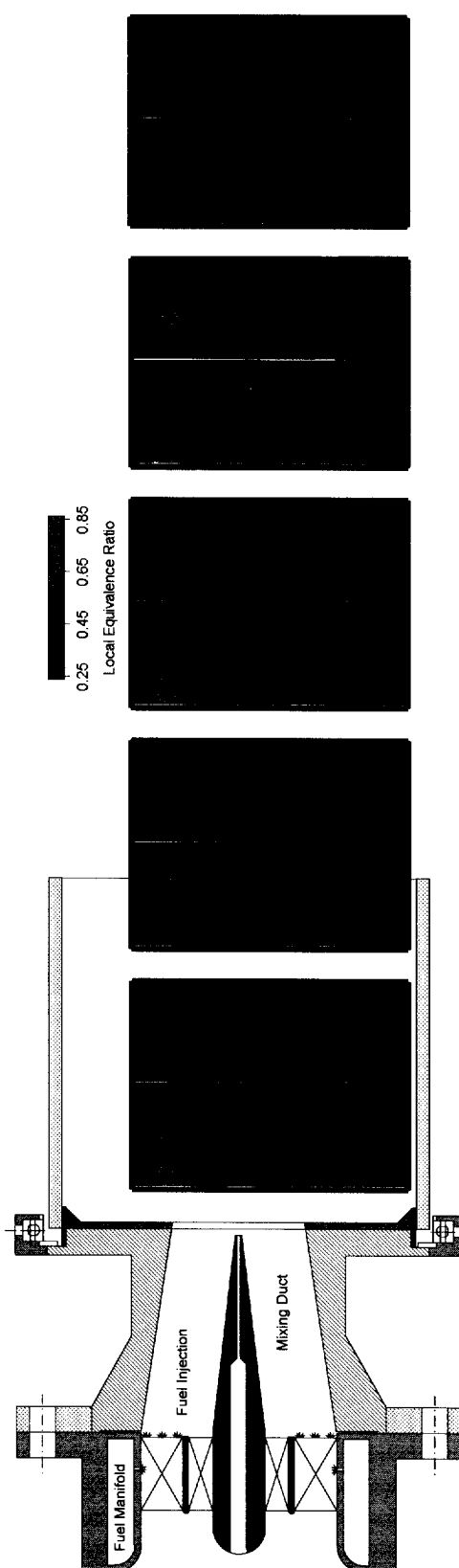


Figure 10. Assembly of four single-shot acetone PLIF results for case II.



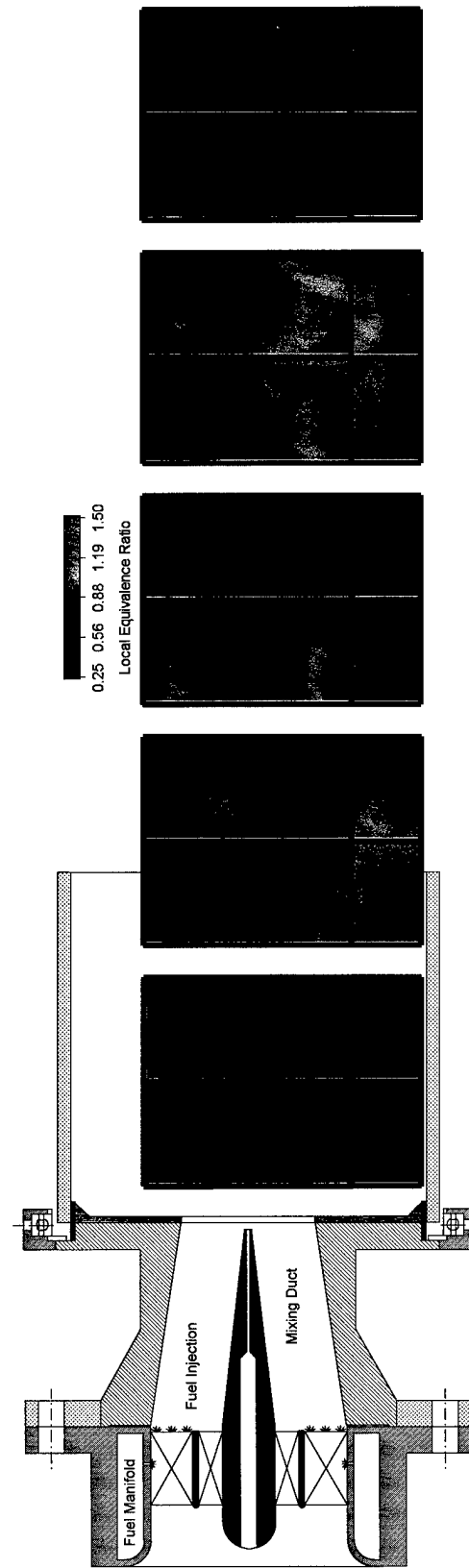


Figure 11. Assembly of four single-shot acetone PLIF results for case III.

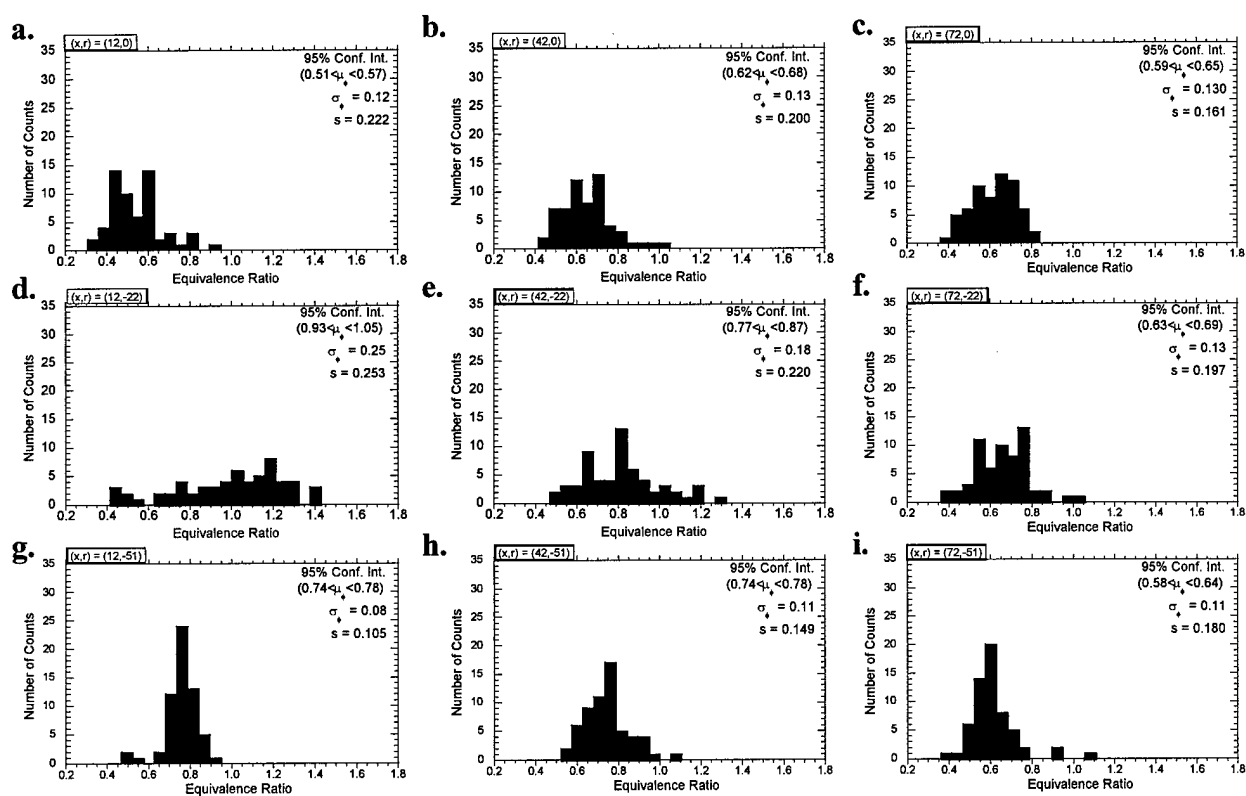
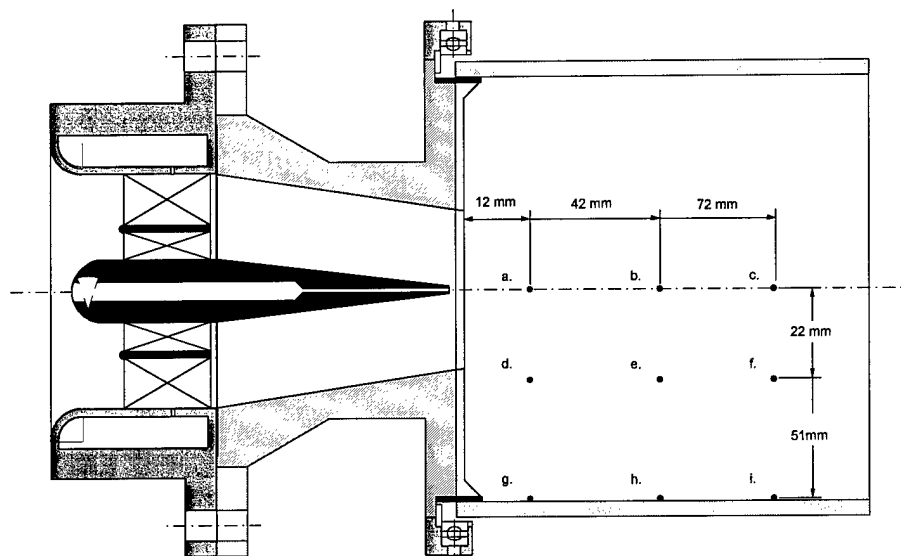


Figure 12. Single-shot point histogram results for case I.

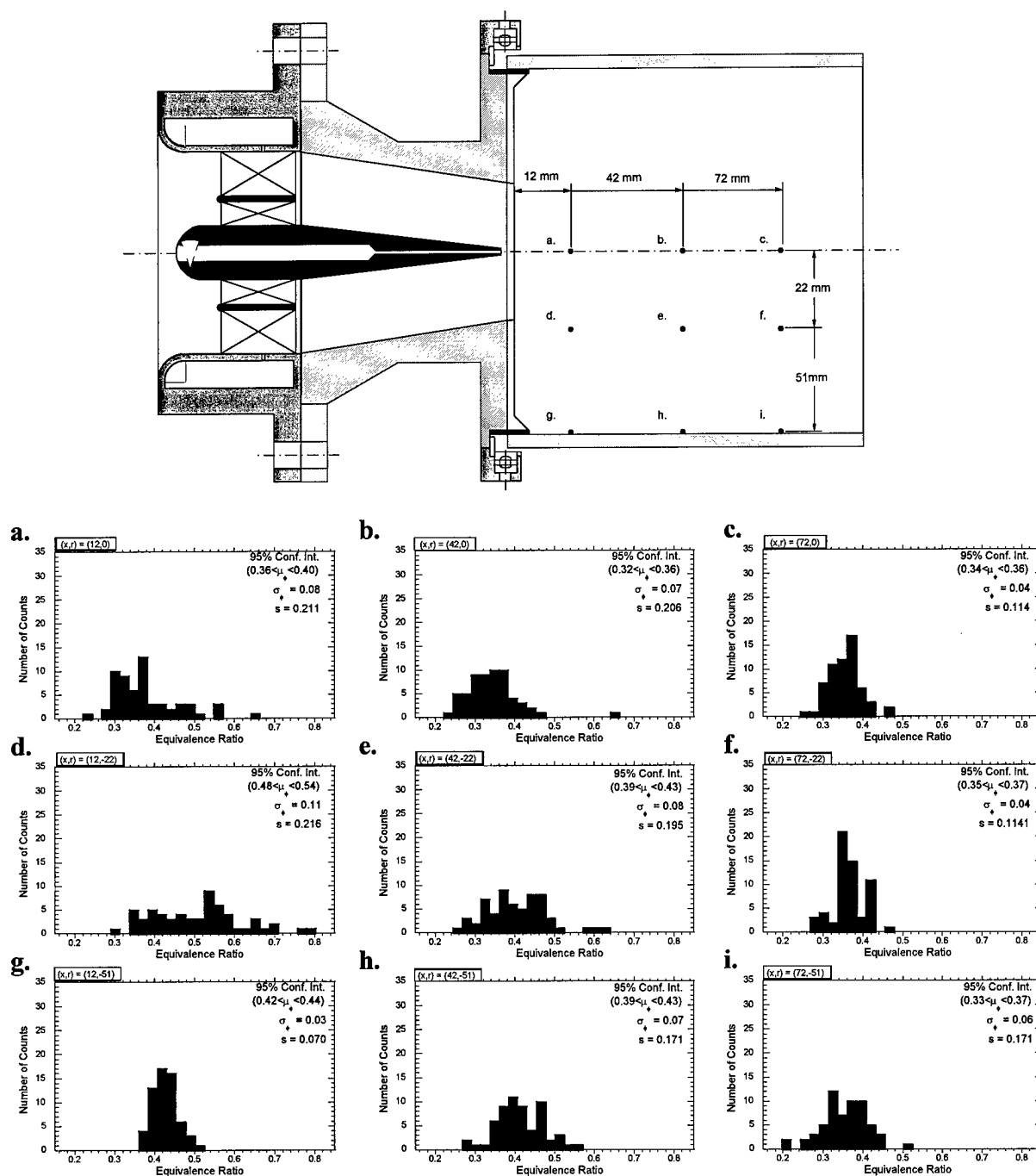


Figure 13. Single-shot point histogram results for case II.

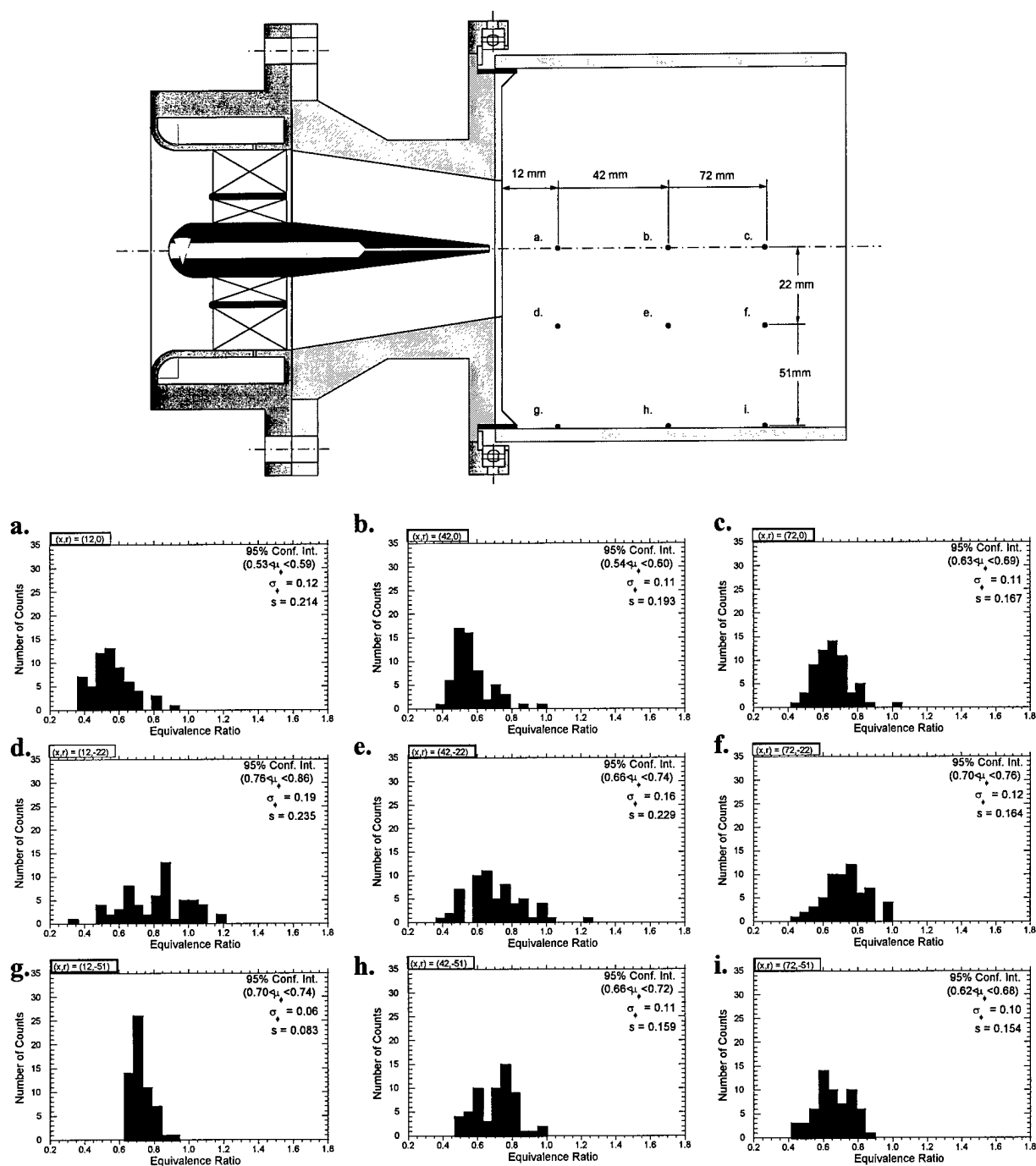


Figure 14. Single-shot point histogram results for case III.

from the outer regions of the premixer cone with significant radial asymmetry. The broad equivalence ratio distributions of the point histograms along the edge of the premixer exit cone (locations d, e and f) indicate the fluctuating nature of these pockets. Histograms taken along the axial centerline for each test condition (locations a, b and c) indicate that the bulk of the central region remains fuel lean. The steep gradients between these fuel-rich and fuel-lean regions persist past the extent of the imaging system. Off-axis recirculation was likely responsible for broadening of the histograms (locations h and i) located along the edge of the combustor 42 mm and 72 mm downstream of the premixer exit face.

The histograms are consistent with the time-averaged images discussed earlier, indicating that test condition I produced the greatest inhomogeneity of the fuel/air distribution. A maximum equivalence ratio of 1.71 was recorded at this condition along the outer edge of the premixer exit cone. Within the same set of images the minimum equivalence ratio measured was 0.46. This degree of unmixedness likely resulted from injecting a majority of the fuel along the outer regions of the premixer manifold.

The single-shot PLIF images obtained at test conditions I and II show comparable large scale structures. The point histograms are also similar with the notable exception of the lower level of unmixedness,  $s$ , for case II at the exit cone of the premixer (locations a and d). As indicated by the 60-shot average, mixing within the premixer cone was improved by lowering the equivalence ratio. The lower equivalence ratio was maintained by decreasing the injection pressure of the gaseous fuel and likely resulted in an increase in the fuel residence time within the premixer.

Comparison of test cases I and III indicates improved mixing as a result of the increase in the air flowrate. The maximum equivalence ratio measured at condition III was 1.48 compared to 1.71 at condition I. Again, point histograms immediately downstream from the premixer exit cone (locations a and d) show lower unmixedness values,  $s$ , for test condition III. Evidently, augmentation of the mixing process by the intensified shear layer between the counter-rotating swirling flows more than offsets the effect of shorter fuel residence times associated with the higher flowrates.

Overall, the temporally resolved acetone PLIF images obtained at the three test conditions each show significant fuel/air unmixedness. However, uniform mixture concentrations were observed in the recirculation regions near the premixer exit face.

### 2.3.2 Cold Flow Mixing Studies: 500 kPa

Mixing studies have been performed at a pressure of 500 kPa to investigate the effect of higher pressure on the premixer performance. The test matrix for these studies is shown in Table 2. For these studies fuel temperature was increased to more closely match the air inlet

temperature, reducing calibration errors due to the temperature dependence of acetone fluorescence. An equivalence ratio of 0.4 was used in the 5% pressure drop tests (VI) due to limitations of the fuel/acetone supply system at high pressure. Therefore, the effect of the pressure drop on flow unmixedness will be assessed by comparing the two low-equivalence-ratio test cases V and VI.

For the 500 kPa measurements, the laser sheet was widened to approximately 45 mm so that the entire visible section of the combustor could be imaged in two axial steps. As with the 100 kPa studies, two radial locations were imaged at each axial location. At each of these four regions, 80 single-shot images were taken to provide slightly better confidence intervals for statistical analysis.

Test Case Number	$P_{\text{comb}}$ (kPa)	$\Delta P_{\text{comb}}$ (%)	$\Phi_{\text{overall}}$	$T_{\text{comb}}$ (K)	$T_{\text{fuel}}$ (K)
IV	500 $\pm 7.5$	3.0 $\pm 0.16$	0.70 $\pm 0.033$	364 $\pm 23$	371 $\pm 25$
V	500 $\pm 8.5$	3.0 $\pm 0.05$	0.40 $\pm 0.026$	365 $\pm 20$	380 $\pm 35$
VI	499 $\pm 8.0$	4.83 $\pm 0.07$	0.41 $\pm 0.018$	360 $\pm 18$	373 $\pm 16$

Table 2. Five-atmosphere test conditions.

Although processing of the high-pressure data is not yet complete, qualitative analysis of the images shows that the increase in pressure does not significantly change the fuel/air mixing. For test cases IV, V, and VI, four unprocessed single-shot images from region 1 (centered along the axis of the premixer, adjacent to the premixer exit face) are shown in Figs. 15, 16, and 17, respectively. Clearly, there is still a large degree of spatial variation and temporal fluctuation in the mixing fields, and the mixing is still dominated by large scale structures. It appears that, as with the low-pressure studies, the level of unmixedness is highest for the low flowrate, high equivalence ratio test case, although further processing will be required to verify this.

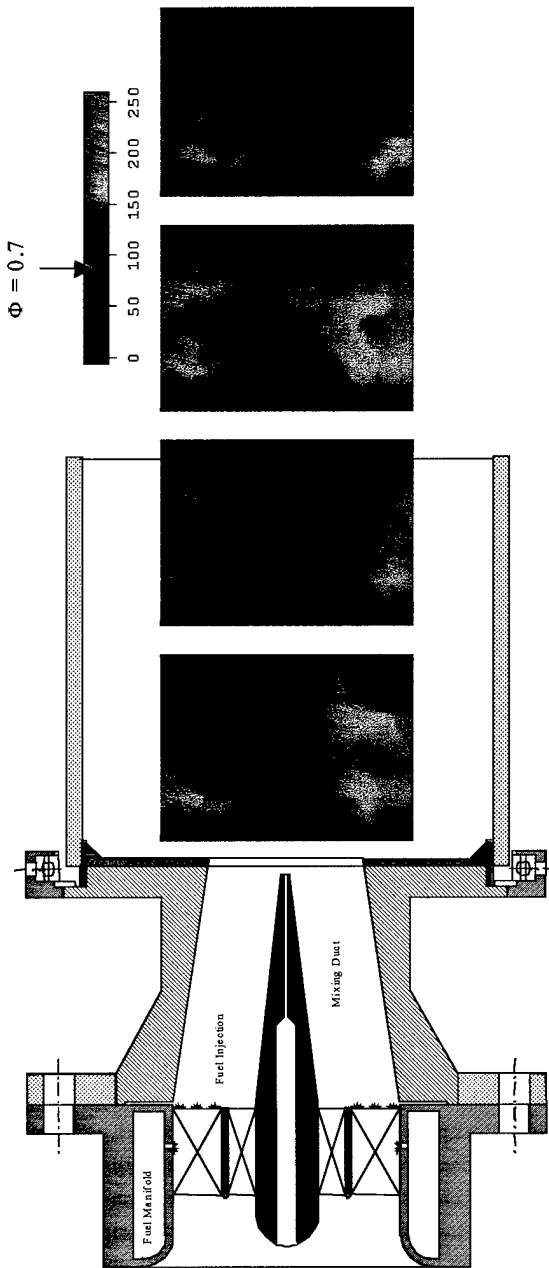


Figure 15. Unprocessed single-shot acetone PLIF images for case IV.

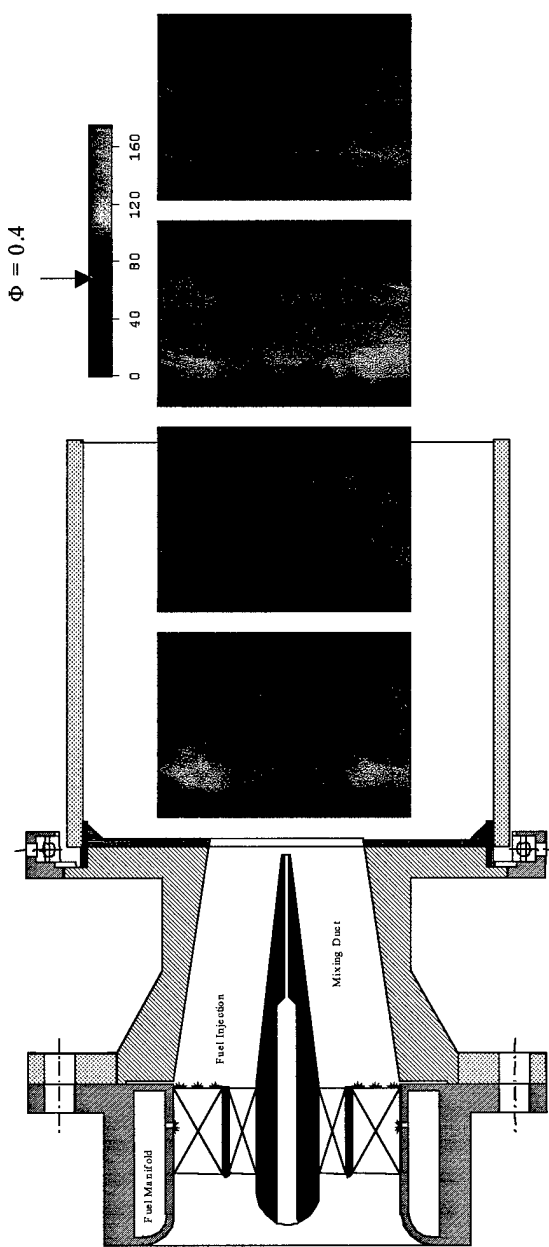


Figure 16. Unprocessed single-shot acetone PLIF images for case V.

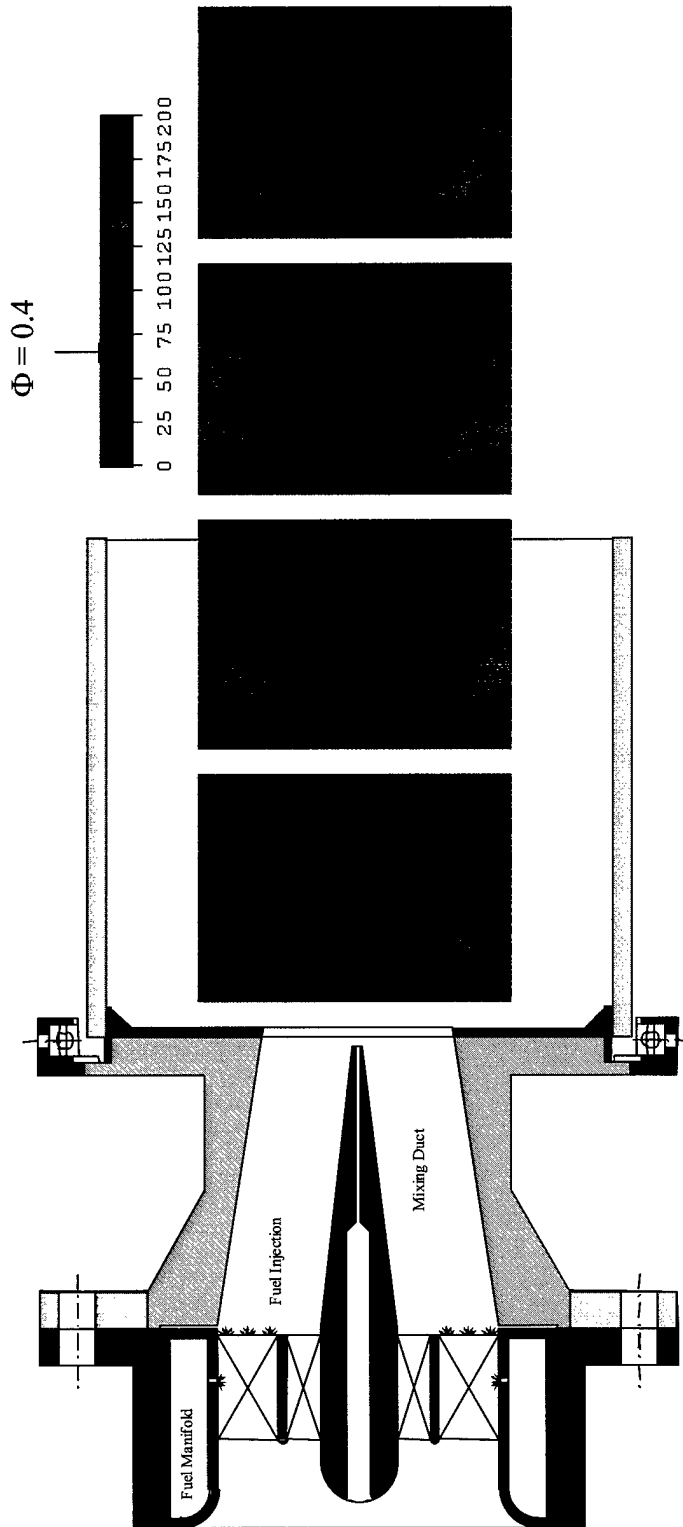


Figure 17. Unprocessed single-shot acetone PLIF images for case VI.



## 2.4 Conclusions and Future Efforts

### 2.4.1 Conclusions

During the three years of the premixed gas turbine project, we have completed the design and constructed a facility that will allow comprehensive optical diagnostics of temperature and species concentrations. 100kPa fuel/air mixing studies using acetone PLIF have been completed during the last year. High pressure mixing studies are underway.

The 100 kPa mixing studies showed significant time-averaged spatial variations near the exit face of the premixer. Local time-averaged maxima in the equivalence ratio peaked at values 51% greater than the overall equivalence ratio. Inhomogeneities were quickly dissipated at downstream locations. Off-axis recirculation was sufficient to provide uniform mixtures close to the overall stoichiometry near the premixer exit face.

By providing two-dimensional instantaneous images of the flow field, single-shot acetone PLIF yielded spatially and temporally resolved information simultaneously. These results indicated that the mixing field was dominated by large-scale structures. As expected, temporal fluctuations in the local equivalence ratio were considerably larger than the spatial variation shown in the time-averaged results. Local instantaneous maxima in the equivalence ratio peaked at values 144% greater than the overall stoichiometry for the high equivalence ratio, low pressure drop case at atmospheric pressure.

High-pressure (500 kPa) fuel-air mixing studies have been performed. Qualitatively, the images show that mixing is not significantly different at these higher pressures compared to the atmospheric pressure results.

### 2.4.2 Future Efforts

Upon completion of the high-pressure fuel-air mixing studies, our comprehensive laser diagnostic combustion measurements will continue. The first laser diagnostic combustion measurements planned are planar OH LIF imaging, which will be accomplished using the 284-nm frequency doubled output of a narrow-band dye laser. This will provide us with statistical information regarding flame front location and guide in the selection of regions of interest for extensive point laser diagnostic investigations. We will then investigate selected regions of the flowfield in great detail using dual-pump CARS to simultaneously probe  $\text{CO}_2$  and  $\text{N}_2$  molecules. These studies will provide accurate spatially and temporally resolved measurements of temperature and relative species concentration, which will identify potential hotspots in the flame, provide further information on the location of the reaction zone, and furnish information on the recirculation of the reaction products.

Subsequently, spatially and temporally resolved measurements of NO and CO will be performed using point-wise LIF. Saturated LIF will be used to obtain quantitative measurements of NO concentration. CO concentrations will be measured using two-photon LIF excited by 230 nm laser radiation also obtained using the frequency doubled output of a narrow-band dye laser.

During all combustion studies, spatially and temporally averaged gas sampling emissions tests of O<sub>2</sub>, HC, NO, CO, and CO<sub>2</sub> will be performed.

## 2.5 References

1. Mikus, T. and Heywood, J. P., "*The Automotive Gas Turbine and Nitric Oxide Emissions*," Combustion Science and Technology **4**, 149-158 (1971).
2. Breuer, G.M. and Lee, E.K.C., "*Fluorescence Decay Time of Cyclic Ketones, Acetone, and Butanal in the Gas Phase*," Journal of Physical Chemistry **75**, 989-990 (1971).
3. Lozano, A., Yip, B. and Hanson, R. K., "*Acetone: A Tracer for Concentration Measurements in Gaseous Flows by Planar Laser-Induced Fluorescence*," Experiments in Fluids **13**, 369-376 (1992).
4. Yuen, L. S., Peters, J. E. and Lucht, R. P., "*Pressure Dependence of Laser-Induced Fluorescence from Acetone*," Applied Optics **36**, 3271-3277 (1997).
5. Thurber, M. C., Grisch, F. and Hanson, R. K., "*Temperature Imaging with Single- and Dual-Wavelength Acetone PLIF*," Optics Letters **22**, 251-253 (1997).

## 3.0 Personnel

The AASERT program supports Mr. Timothy R. Frazier, a Ph.D. candidate (and U.S. citizen) and Mr. John J. Stephens, an undergraduate (and U.S. citizen). The co-principal investigators on the project are Professor James E. Peters and Professor Robert P. Lucht.

## 4.0 Publications

No peer-reviewed publications during the reporting period of August 1, 1997 to July 31, 1998.

## 5.0 Interactions/Transitions

Frazier, Timothy R., Robert E. Foglesong, Robert E. Coverdill, James E. Peters, and Robert P. Lucht, "An Experimental Investigation of Fuel/Air Mixing in an Optically Accessible Axial Premixer," Presented at the 34th AIAA/ASME/SAE/ASEE Joint Propulsion Conference and Exhibit, July 13-15, 1998, Cleveland, Ohio.

**6.0 Discoveries, inventions and/or disclosures**

There were no discoveries, inventions or patent disclosures during the reporting period of August 1, 1997 to July 31, 1998.

**7.0 Honors/Awards**

R. P. Lucht was named a Fellow of the OSA in 1998. J. E. Peters was named an Associate Fellow of the AIAA in 1991 and a Fellow of ASME in 1997.

## 15

PI DATA

FY \_\_\_\_\_

Volume \_\_\_\_\_ Page(s) \_\_\_\_\_ Month Published \_\_\_\_\_ Year Published \_\_\_\_\_

HONORS/AWARDS RECEIVED DURING CONTRACT/GRANT LIFETIME

Include: All honors and awards received during the lifetime of the contract or grant, and any life achievement honors such as (Nobel prize, honorary doctorates, and society fellowships) prior to this contract or grant.

Do Not Include: Honors and awards unrelated to the scientific field covered by the contract/grant.

Honor/Award Fellow Year Received: 1998  
Honor/Award Recipient(s) R. P. Lucht  
Awarding Organization OSA

Honor/Award Associate Fellow Year Received: 1991  
Honor/Award Recipient(s) J. E. Peters  
Awarding Organization AIAA

Honor/Award Fellow Year Received: 1997  
Honor/Award Recipient(s) J. E. Peters  
Awarding Organization ASME

**AUGMENTATION AWARDS FOR SCIENCE & ENGINEERING RESEARCH TRAINING (AASERT)**  
**REPORTING FORM**

The Department of Defense (DoD) requires certain information to evaluate the effectiveness of the AASERT Program. By accepting this Grant which bestows the AASERT funds, the Grantee agrees to provide 1) a brief (not to exceed one page) narrative technical report of the research training activities of the AASERT-funded student(s) and 2) the information requested below. This information should be provided to the Government's technical point of contact by each annual anniversary of the AASERT award date.

1 Grantee identification data: (R&T and Grant numbers found on Page 1 of Grant)

- a University of Illinois  
University Name
- b F49620-97-1-0456  
Grant Number
- c FQ8671-9701160  
R&T Number
- d J. E. Peters and R. P. Lucht  
PI Name
- e From: Aug. 1, 1997 To: July 31, 1998  
AASERT Reporting Period

NOTE Grant to which AASERT award is attached is referred to hereafter as "Parent Agreement".

2 Total funding of the Parent Agreement and the number of full-time equivalent graduate students (FTEGS) supported by the Parent Agreement during the 12-month period prior to the AASERT award date.

- a Funding \$ \$256,382
- b Number FTEGS 1

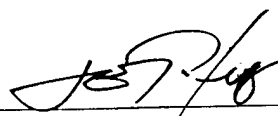
3 Total funding of the Parent Agreement and the number of FTEGS supported by the Parent Agreement during the current 12-month reporting period

- a Funding \$ \$41,578
- b Number FTEGS 0

4 Total AASERT funding and the number of FTEGS and undergraduate students (UGS) supported by AASERT funds during the current 12-month reporting period

- a Funding \$ \$47,809
- b Number FTEGS 1
- c Number UGS 1

VERIFICATION STATEMENT I hereby verify that all students supported by the AASERT award are U.S. citizens

  
Principal Investigator

August 28, 1998  
Date